Development 140, 886-896 (2013) doi:10.1242/dev.086546

Hepatocyte nuclear factor 1β controls nephron tubular development

Filippo Massa[1], Serge Garbay[1], Raymonde Bouvier[2], Yoshinobu Sugitani[3], Tetsuo Noda[3], Marie-Claire Gubler[4], Laurence Heidet[5], Marco Pontoglio[1,*] and Evelyne Fischer[1,*]

SUMMARY

Nephron morphogenesis is a complex process that generates blood-filtration units (glomeruli) connected to extremely long and patterned tubular structures. Hepatocyte nuclear factor 1β (HNF1β) is a divergent homeobox transcription factor that is expressed in kidney from the first steps of nephrogenesis. Mutations in *HNF1B* (OMIM #137920) are frequently found in patients with developmental renal pathologies, the mechanisms of which have not been completely elucidated. Here we show that inactivation of *Hnf1b* in the murine metanephric mesenchyme leads to a drastic tubular defect characterized by the absence of proximal, distal and Henle's loop segments. Nephrons were eventually characterized by glomeruli, with a dilated urinary space, directly connected to collecting ducts via a primitive and short tubule. In the absence of HNF1β early nephron precursors gave rise to deformed S-shaped bodies characterized by the absence of the typical bulge of epithelial cells at the bend between the mid and lower segments. The lack of this bulge eventually led to the absence of proximal tubules and Henle's loops. The expression of several genes, including *Irx1*, *Osr2* and *Pou3f3*, was downregulated in the S-shaped bodies. We also observed decreased expression of *Dll1* and the consequent defective activation of Notch in the prospective tubular compartment of comma- and S-shaped bodies. Our results reveal a novel hierarchical relationship between HNF1β and key genes involved in renal development. In addition, these studies define a novel structural and functional component of S-shaped bodies at the origin of tubule formation.

KEY WORDS: HNF1β, MODY5, Notch pathway, Kidney development, CAKUT

INTRODUCTION

Kidney development is a tightly regulated morphogenic process based on crosstalk between the metanephric mesenchyme (MM) and ureteric bud (UB) (Dressler, 2009). Any dysfunction in this process may lead to a variety of congenital abnormalities of the kidney and urinary tract (CAKUT) (Rumballe et al., 2010). Depending on the nature of the affected compartment, abnormalities in the differentiation program can lead to defects ranging from kidney agenesis to urinary tract malformations.

One of the most prevalent genetic defects responsible for this complex pathology is represented by mutations in the gene that encodes hepatocyte nuclear factor 1β (*HNF1B*), a divergent homeobox transcription factor. *HNF1B* mutations are detected in ~20-30% of patients or fetuses that suffer from renal developmental anomalies, predominantly including renal cysts, hypoplasia or single kidneys (Decramer et al., 2007; Heidet et al., 2010; Ulinski et al., 2006). Even though mutations in *HNF1B* are known to be responsible for maturity-onset diabetes of the young (MODY) type 5 (Horikawa et al., 1997; Lindner et al., 1999), several studies have consolidated the idea that one of first traits of pediatric patients and fetuses carrying *HNF1B* mutations is represented by the occurrence of renal malformations (Decramer et al., 2007; Heidet et al., 2010; Ulinski et al., 2006).

The study of animal models for *Hnf1b* deficiency in renal development and maturation has helped us to understand some of the functions of HNF1β (Bohn et al., 2003; Gresh et al., 2004; Hiesberger et al., 2004; Lokmane et al., 2010; Sun et al., 2004; Verdeguer et al., 2010; Wu et al., 2004). The phenotype of mice lacking *Hnf1b* depends very much on exactly when (developmental timing) and where (which tissue compartment) the gene is inactivated. For instance, it has been shown that germline inactivation of *Hnf1b* is embryonic lethal (E7.5) (Barbacci et al., 1999; Coffinier et al., 1999a). During kidney development, the lack of this gene in the UB leads to defective UB branching and to the absence of mesenchymal to epithelial transition due to defective expression of key genes including *Wnt9b* (Lokmane et al., 2010) (our unpublished observations). In parallel, it has been shown that deletion of *Hnf1b* in already formed, still elongating, tubular segments leads to a severe polycystic kidney phenotype (Gresh et al., 2004; Verdeguer et al., 2010). In this context, it has been demonstrated that HNF1β is a bookmarking factor that is required for postmitotic reprogramming of the expression of a number of genes whose mutation is frequently associated with cystic kidney disease (Verdeguer et al., 2010). In addition, we have shown that the tubular elongation of nephrons during their postnatal maturation is due to the particular orientation of mitotic spindles. This mitotic alignment is lost in the renal cystic epithelium (Fischer et al., 2006).

In recent years a considerable number of studies have clarified the key molecular mechanisms involved in the first steps of nephron morphogenesis (Boyle et al., 2011; Carroll et al., 2005; Cheng et al., 2007; Stark et al., 1994). However, the signaling pathways and the actors that specify the identity and expansion of tubules in nephron precursors are still mostly unknown. Recent studies have highlighted the crucial role of the Notch signaling pathway in tubular segmentation and glomerular formation. The inactivation of *Notch2*,

[1]Expression Génique, Développement et Maladies (EGDM) Team, INSERM U1016, CNRS UMR 8104, Université Paris-Descartes. Institut Cochin; Département de Génétique et Développement, 75014 Paris, France. [2]Hospices civils de Lyon, Centre de pathologie Est, 69677 Bron Cedex, France. [3]Department of Cell Biology, Cancer Institute, The Japanese Foundation for Cancer Research, 3-8-31 Ariake, Koto-ku, Tokyo 135-8550, Japan. [4]INSERM U983, Hôpital Necker-Enfants Malades, 75015 Paris, France. [5]AP-HP, Centre de Référence MARHEA, Service de Néphrologie Pédiatrique, Hôpital Necker-Enfants Malades, 75015 Paris France.

*Authors for correspondence (marco.pontoglio@inserm.fr; evelyne.fischer@inserm.fr)

Accepted 26 November 2012

one of the Notch receptors, in renal mesenchyme is responsible for the absence of both proximal tubular formation and glomerulogenesis. In addition, a hypomorphic allele of one of its ligands, delta-like 1 (Dll1), is responsible for a drastic defect in proximal tubular formation (Cheng et al., 2007).

Nephron tubular compartments are generated by a proliferative expansion of presumptive tubular cells that emerge from S-shaped bodies. At the morphological level, these nephron precursors are composed of three distinct segments: the upper limb, which will give rise to the distal convoluted tubule (DCT), the mid-limb, which will generate Henle's loop (HL) and proximal tubule (PT) segments; and the lower limb, which will form the blood filtration unit of the nephron, the glomerulus. Recently, analysis of the expression pattern of specific developmental genes has shown that the mid-limb can be further subdivided into specific domains (Thiagarajan et al., 2011; Yu et al., 2012). However, the biological significance of this fine-tuned, patterned gene expression, along with the actual developmental functions of these domains, remain poorly explored.

In the present study, we demonstrate that the lack of HNF1β in the MM leads to the formation of aberrant nephrons that are characterized by glomeruli with a dilated Bowman's space and that lack their typical tubular components. Mutant S-shaped bodies were characterized by the absence of a bulge of epithelial cells in the mid-limb. We show that this phenotype is linked to the defective expression of *Irx1*, *Osr2* and *Pou3f3* and to defective Notch signaling activation associated with a downregulation of *Dll1*.

MATERIALS AND METHODS

Mice

Specific inactivation of *Hnf1b* in the MM was obtained using a Cre-loxP strategy. *Six2-Cre* (Kobayashi et al., 2008), $Hnf1b^{lacZ/+}$ and $Hnf1b^{f/f}$ mice were described previously (Coffinier et al., 2002; Coffinier et al., 1999b). Since *Six2-Cre;* $Hnf1b^{f/+}$ or *Six2-Cre;* $Hnf1b^{lacZ/+}$ mice were indistinguishable from wild-type mice, all these animals are indicated in this study as 'controls'. Inactivation of *Notch2* was achieved with a floxed allele $Notch2^{tm3Grid}$ and/or with a null allele described previously (BayGenomics, San Francisco, CA, USA) (Tan et al., 2009). The inactivation of *Pou3f3* was described previously (Nakai et al., 2003). Animals were maintained in two animal facilities, each of which is licensed by the French Ministry of Agriculture (agreement A 75-14-02, dated April 24, 2007). All experiments conformed to the relevant regulatory standards.

Tissue sample preparation and immunohistochemistry

Human fetal renal specimens and fetal tissue for DNA isolation were collected after obtaining informed consent from the parents. The pregnancy had been interrupted during the third trimester because of cystic kidneys, following parental request and acceptance by the Prenatal Diagnosis Center of Lyon (France). Genomic DNA was isolated by standard methods. Mutation screening was performed as described (Heidet et al., 2010). Images of histological sections from a MODY5 patient carrying a c.232G>T, p.Glu78X mutation were provided by Professor Laurent Daniel, CHU Timone, Marseille, France.

Mouse kidneys were dissected from embryos at E13.5, E14.5, E16.5 and E18.5 and from newborn pups (P0). Histological and immunohistochemical analyses were performed on 5 µm paraffin sections. After antigen retrieval in boiling citrate buffer (Dako, S2369) for 15 minutes, sections were treated with the MOM Kit (Vector Labs, BMK-2202) according to the manufacturer's instructions and incubated with antibodies (supplementary material Table S1) for 1 hour at room temperature or at 4°C overnight. After several washes in PBS containing 0.1% Tween 20 (PBST), samples were incubated with Alexa Fluor-conjugated secondary antibodies (Invitrogen; 1:500) for 1 hour at room temperature. Sections were analyzed with a Leica microscope equipped with a Yokogawa CSU-X1M1 spinning disk. Images were analyzed with ImageJ (NIH).

In situ hybridization (ISH)

cDNA from genes of interest was obtained by reverse transcription followed by PCR amplification using specific primers (supplementary material Table S2). The templates were either subcloned into pGEM7Z(+) Vector (Promega) or used directly as templates with a specific SP6 or T7 tail to generate digoxigenin-labeled RNA probes with the Digoxigenin RNA Labeling Kit (Roche). ISH experiments were carried out as described (D'Angelo et al., 2010).

Quantitative real-time (RT)-PCR analysis

cDNA was obtained from total RNA from E13.5, E14.5 and P0 kidneys of control and mutant animals using the SuperScript III Reverse Transcriptase Kit (Invitrogen, 18080-051). Gene expression was analyzed by quantitative (q) PCR using the Stratagene Mx3000P Real-time PCR System with SYBR Green-Rox (Roche, 04 913 914 001) in triplicate. Primers (supplementary material Table S3) were designed using Primer3 software (simgene.com/Primer3). Expression levels in mutants are indicated relative to controls. Results were normalized to the Gapdh expression level. n=3 for control and mutant at E13.5 and P0; n=5 for control and mutant at E14.5.

Chromatin immunoprecipitation (ChIP)

Nuclei were purified from pooled wild-type embryonic kidneys. Chromatin preparation and ChIP were performed as described (Verdeguer et al., 2010). Quantification of precipitated specific DNA fragments was carried out by qRT-PCR in triplicate. Relative fold-enrichment of DNA fragments was calculated using the following formula: ChIP HNF1β/ChIP IgG. Primers (supplementary material Table S4) were designed using Primer3 software.

Assessment of the extent of proliferation and apoptosis

To evaluate proliferation and apoptosis, 100 µm vibratome sections were postfixed for 10 minutes in 4% paraformaldehyde at room temperature and then incubated with peanut agglutinin (Vector Labs, RL-1072) and anti-cleaved caspase-3 antibody (R&D Systems, AF835) or anti-phosphorylated histone H3 antibody (Abcam, Ab5819) for 48 hours in PBS containing 0.1% sodium azide and 0.01% Triton X-100.

Electron microscopy

Kidneys were cut into 1 mm^3 slices, fixed for 1 hour in 3% glutaraldehyde and postfixed in 1% osmium oxide. EPON resin-embedded samples were then cut (70 nm ultrathin sections) with a Reichert Ultracut S ultramicrotome and analyzed with a JEOL 1011 electron microscope.

RESULTS

HNF1β deficiency in the metanephric mesenchyme results in early postnatal lethality

To analyze the role played by HNF1β in nephrogenesis we used a Cre mouse strain that selectively inactivates *Hnf1b* in nephron progenitor mesenchymal cells. SIX2 is a transcription factor that is specifically expressed in mesenchymal stem cells that give rise to all nephron epithelial cells (Kobayashi et al., 2008). It has been shown that *Six2-Cre* transgenic animals (Humphreys et al., 2008) target this stem cell compartment without affecting the UB. With this strategy, embryos carrying an $Hnf1b^{f/f}$*; Six2-Cre* germline genotype should maintain the expression of HNF1β in the UB, which in turn should provide the mesenchyme with all the signaling stimuli necessary for the mesenchymal to epithelial transition (MET) at the origin of nephrogenesis.

Our results showed that MM-specific *Six2-Cre*-driven *Hnf1b*-deleted embryos (indicated here as 'mutant' embryos) did not suffer from any prenatal lethality and were delivered at the expected Mendelian ratio. However, newborns died between the first and second day after birth (Table 1), a lifespan compatible with severe kidney failure. Macroscopic examination showed that kidneys from mutant newborns were small, with a length ~70% of that of control littermates (Fig. 1A,B). Consistently, the bladder of mutant embryos

Table 1. Early postnatal lethality in *Hnf1b* mutants

Age	Controls	Mutants	Total
E14.5-16.5	75	24	99
E17.5-18.5	47	20	67
P0	22	8	30
P1	51	19	70
P2	46	10‡	56
P>2	48	0**	48

Six2-Cre-mediated inactivation of *Hnf1b* does not lead to embryonic lethality: mutants and controls (wild-type and *Hnf1b*$^{+/-}$ pups or embryos) were present at a normal Mendelian ratio during gestation. Newborn pups lacking *Hnf1b* in the metanephric mesenchyme survived until birth, but they died during the first 48 hours of life. ‡Mice found dead. ***P*<0.01.

was small, suggesting that pups were unable to produce normal levels of urine (Fig. 1C,D). In addition, 15% of newborn pups showed hydroureter and hydronephrosis (data not shown).

Expression of HNF1β in nephron precursors is essential for the development of tubules

At birth, the nephrogenic zone, which is localized in the more external part of the cortex, was of similar thickness in mutant and control kidneys. However, the typical convoluted tubular epithelial structures that are normally visible in the cortex were absent in mutant kidneys (Fig. 1E,F).

In order to characterize the identity of the missing tubular segments, we performed immunostaining and *in situ* hybridization (ISH) on renal histological sections. Our results showed that, at birth, mutant pups lacked most of the tubular nephron segments that are typically produced by the nephrogenic mesenchyme. In particular, mutant embryos showed a very drastically reduced production of PTs, HLs and DCTs. The use of *Lotus tetragonolobus* lectin (LTL) showed only rare, scattered PTs (Fig. 1G,H). In a similar way, only very rare HLs and DCTs were detected, as shown by the almost complete lack of *Slc12a1* (*Nkcc2*) and parvalbumin (*Pvalb*) expression (Fig. 1I-L). In addition, qRT-PCR demonstrated that, at P0, mutant pups had a dramatic decrease in the expression of several mRNAs normally expressed in the PT, HL and DCT (Fig. 1M).

In agreement with the absence of Cre expression in the UB, the collecting ducts (CDs) were unaffected, as demonstrated by the presence of the typical medullar tubular rays in mutant newborn pups (Fig. 1E,F). In addition, immunochemistry, immunofluorescence and qRT-PCR experiments showed that all these tubules were positive for typical markers of CDs, such as *Dolichos biflorus* agglutinin (DBA) staining (supplementary material Fig. S1A,B) and *Wnt9b* (supplementary material Fig. S1E) and remained positive for the expression of HNF1β (Fig. 2).

Interestingly, the absence of HNF1β did not significantly impair the differentiation of cell types in glomeruli. Consistent with these findings, podocytes expressed normal levels of *Wt1* (supplementary material Fig. S1C,D). Nevertheless, these glomeruli presented with an abnormal shape (see below) and several exhibited visible dilation of the Bowman's capsule (Fig. 1E,F, inset).

Taken together, these observations demonstrated that, in the absence of HNF1β, nephron precursors were somehow able to form glomerular structures but were not competent to generate and expand tubules.

Drastic distortion of nephron precursors in the absence of HNF1β

In order to characterize the mechanisms underlying the phenotypes observed we aimed to identify the first detectable abnormalities that led to these drastic developmental defects. In agreement with previous studies (Harding et al., 2011; Lokmane et al., 2010; McMahon et al., 2008), immunofluorescence experiments showed that HNF1β was not expressed in cap mesenchyme (Fig. 2A, arrow). HNF1β was first detected in renal vesicles, with a clear polarized distal pattern in a limited number of cells adjacent to the UB, in the prospective tubular compartment (Fig. 2A). The first steps of MET were preserved in kidney from embryos carrying a *Six2-Cre*-driven *Hnf1b* deletion (Fig. 2B). In addition, the characteristic mutually exclusive distal/proximal expression pattern of specific genes (Georgas et al., 2008) was preserved. In both control and mutant embryos, vesicles were characterized by polarized expression of *Jag1* in the distal portion of the vesicle, whereas *Wt1* expression was restricted to the proximal compartment (Fig. 2C,D) (Georgas et al., 2008).

In mutant embryos, comma-shaped bodies did not display any detectable morphological abnormalities, whereas the structure of S-shaped bodies was significantly altered. In control embryos, HNF1β was expressed at high levels in the prospective tubular segments of comma- and S-shaped bodies (Fig. 2E,G). Of note, HNF1β was expressed in the prominent and protruding bulge of epithelial cells that forms the first bend between the mid and the lower limb, clearly visible in sagittal sections. In the absence of HNF1β, this typical structure did not form (Fig. 2G,H,K-N). In coronal sections of S-shaped bodies of control embryonic kidneys, we observed the mid-limb cut in a perpendicular orientation, almost circular in shape. This structure is typically positioned over a concentric, concave layer of columnar epithelial cells that are strongly positive for *Wt1* (which gives rise to the typical podocyte precursor 'smiling' crown) (Fig. 2I). In mutant embryos, this stereotypical 'smiling' structure was replaced by a 'mustached' configuration (Fig. 2J). Mutant embryonic 'S-shaped' structures were characterized by the presence of a mid-limb that was directly connected to the prospective urinary space in the lower limb compartment. In spite of this drastic defect, the most proximal part of the S-shaped body (lower limb) developed normally, giving rise to precursors of podocytes and Bowman's capsule epithelial cells, as illustrated by the expression of *Wt1* (Fig. 2L). The unaltered structure of the lower limb in mutant embryos correlated with the complete absence of HNF1β expression in podocytes and their precursors (Fig. 2G).

In summary, these results showed that the absence of HNF1β in nephron precursors prevented the formation of the prominent and protruding bulge of epithelial cells at the bend between the mid and lower limbs.

Lack of HNF1β prevents the initiation of tubular differentiation

It is known that the emergence, expansion and first differentiation of PTs and HLs begin in the more advanced and mature S-shaped bodies already at E14.5. In qRT-PCR assays on cDNA prepared from total kidneys of control embryos we detected the expression of typical tubular markers (*Hnf1a*, *Hnf4a*, *Vil1* and *Slc12a1*) already at this stage. Their expression further increased just before birth (Fig. 3A, Fig. 2). In agreement with the defective tubule formation and expansion visible in newborns, the expression of all these markers was drastically decreased in mutant embryos already at E14.5 (Fig. 3B).

Most of these genes are known to contain several HNF1 binding sites in their transcriptional control regions (Tronche et al., 1997) (M.P. and S.G., unpublished). The defective expression of these genes might have been ascribed to a potential direct transcriptional

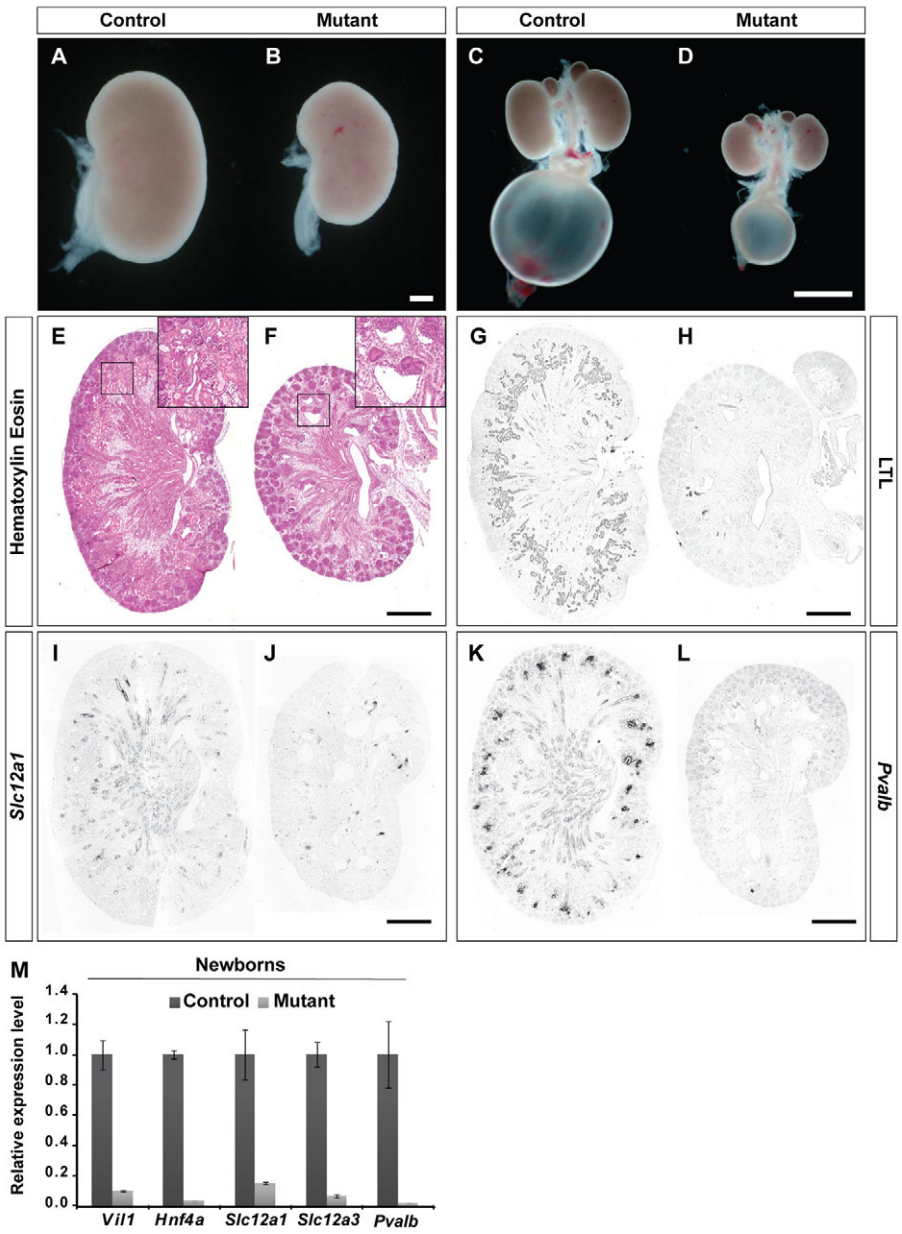

Fig. 1. The absence of HNF1β in nephron precursors leads to smaller kidneys and prevents the formation of tubules. (**A-D**) Macroscopic view of newborn mouse kidneys (A,B) and urinary tract (C,D) showing 30% reduction in the size of *Hnf1b*-deficient kidneys. (**E-L**) Histological sections of newborn mouse kidneys showing a drastic tubular defect in *Hnf1b* mutant pups. (E,F) Hematoxylin and Eosin staining. Boxed areas are magnified in insets and highlight the presence of cystic glomeruli in the mutant. (G,H) *Lotus tetragonolobus* lectin (LTL) staining. (I-L) *In situ* hybridization (ISH) for (I,J) *Slc12a1* (*Nkcc2*) and (K,L) *Pvalb*. (**M**) qRT-PCR analysis for tubular markers at P0. Error bars indicate s.e.m. Scale bars: 100 μm in A,B; 1 mm in C,D; 500 μm in E-L.

activation effect of HNF1β. The concomitant loss of expression of all these genes could have contributed to the aberrant formation and expansion of nephron tubular components. However, in agreement with previous observations (Harding et al., 2011; McMahon et al., 2008), our inspection clearly revealed that S-shaped bodies in wild-type embryos were still devoid of significant expression (protein or mRNA) of these genes. *Hnf1a*, *Hnf4a* and *Vil1* were expressed only at later developmental steps of differentiation and specifically when PTs have already emerged from S-shaped bodies (Fig. 3C; data not shown). Since mutant embryo 'S-shaped' bodies never expanded these tubular structures, we concluded that the defective expression of these genes was simply a consequence, and not the origin, of the developmental defect.

Altogether, these experiments indicated that the absence of tubular components in mutant newborn animals is not due to a progressive loss of normally differentiated tubules. Our results indicated that, in the absence of *Hnf1b*, the process of tubular expansion and differentiation was completely impaired.

The effect of *Hnf1b* deficiency on proliferation and apoptosis

The aberrant conformation of mutant S-shaped structures might have been ascribed to a defective proliferation/apoptotic balance in the precursors of S-shaped bodies (vesicle or comma-shaped bodies). To evaluate this possibility we monitored and compared the occurrence of proliferative and apoptotic events by counting the number of phosphohistone H3 PS10-positive and cleaved caspase-3-positive cells, respectively. This scoring was performed in 100 μm vibratome sections in order to evaluate the occurrence of proliferative and apoptotic events in structures throughout their whole extent. These experiments showed that mutant S-shaped bodies exhibited significantly decreased proliferation specifically in the upper and mid-limbs. These segments were also characterized by a significantly increased number of apoptotic events (Fig. 3D,E).

In the lower limb, we did not see any difference in the average number of proliferative or apoptotic events. This observation paralleled the fact that, in the lower limb, *Hnf1b* is not expressed in

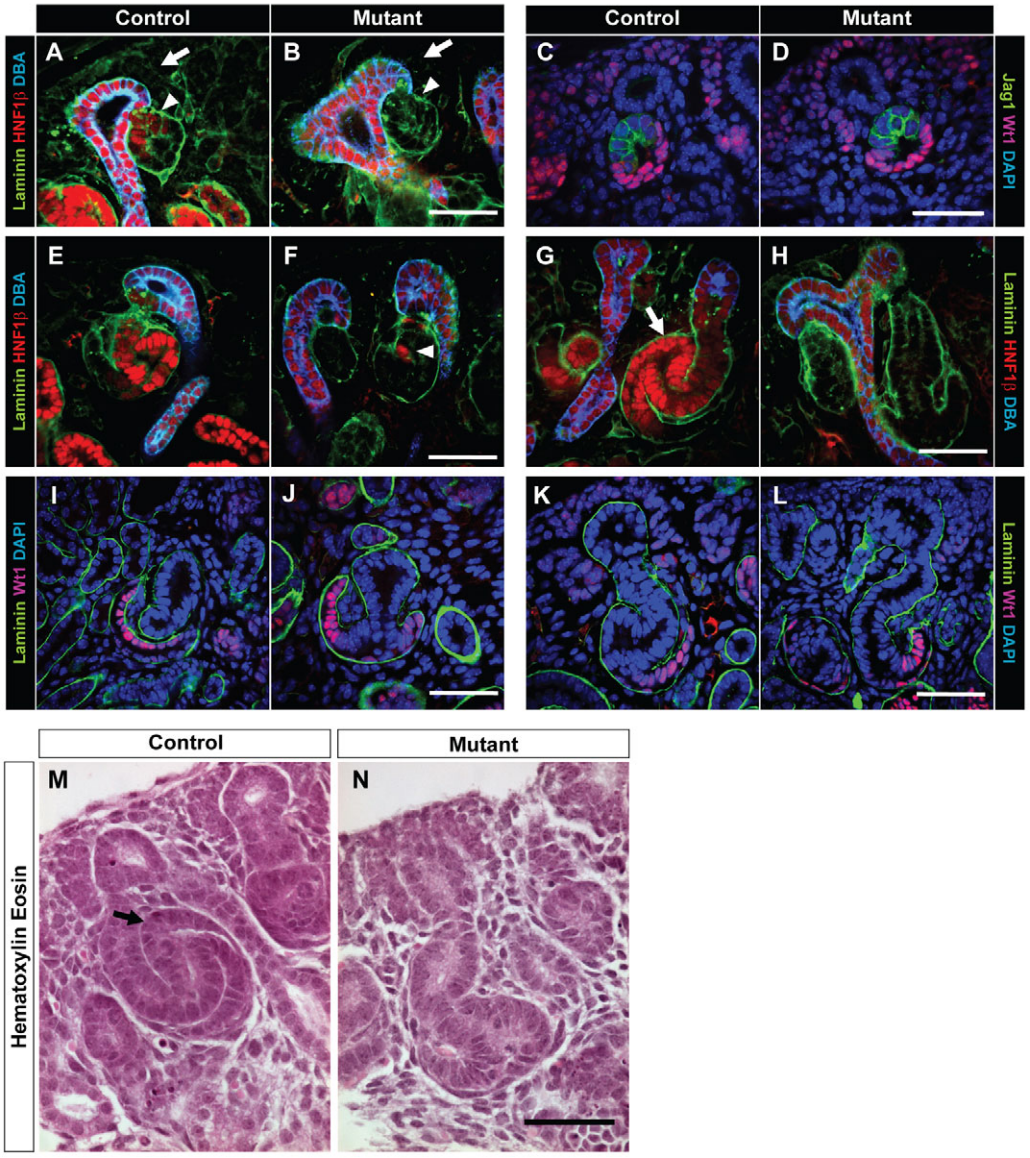

Fig. 2. The absence of HNF1β does not affect the first steps of nephrogenesis, but is responsible for the distortion of S-shaped bodies. (**A**,**B**) Detection of HNF1β in nephron precursors by immunofluorescence. Polarized (distal) expression of HNF1β is visible in vesicles of control embryos (red nuclei, arrowhead in A), whereas it is absent in vesicles of mutant embryos (arrowhead in B). Cap mesenchymal cells do not express HNF1β (arrow in A,B). (**C**,**D**) Mutant vesicles show polarized expression of *Jag1* and *Wt1* that is similar to that of control embryos. (**E**,**F**) Mutant comma-shaped bodies do not display any detectable abnormalities. Sporadically, chimeric residual expression of HNF1β in mesenchyme-derived structures is observed in mutant embryos (e.g. the nucleus indicated by the arrowhead in F). A comparable expression of HNF1β (red) is seen in the non *Six2-Cre*-deleted UB (stained with DBA in blue) in mutant and controls (A,B,E-H). (G-L) Mutant embryos suffer from a drastic deformation of S-shaped structures. (**G**,**H**) Sagittal sections of S-shaped bodies. HNF1β expression in control embryos (G) is particularly strong in the bulge of epithelial cells that is located at the bend between the mid and lower limbs (arrow). This structure is drastically reduced in mutant embryos (H). (**I-L**) Coronal and sagittal sections of S-shaped bodies showing that in mutant embryos the mid-limb is inserted directly into the prospective urinary space, delimited above by *Wt1* highly positive cells (podocyte precursors with red nuclei) and below by capsular cells (which express *Wt1* at low level). (**M**,**N**) Hematoxylin and Eosin staining of sagittal sections of S-shaped bodies. The arrow in M points to the bulge that is missing in mutants. Scale bars: 25 μm.

podocyte precursors and is expressed only at low levels in the prospective capsular cells.

It is worth noting that early nephron precursors (vesicles and comma-shaped bodies) were unaffected by any defective proliferation or excessive apoptosis. Aberrations in these processes only occurred in already deformed S-shaped segments (Fig. 3D,E). This indicated that the defective proliferation and excessive apoptosis can very likely be ascribed to late, secondary effects, possibly linked to the deformation or to the lack of differentiation induced by the absence of HNF1β.

Molecular mechanisms of defective tubule specification

Recent studies have clearly indicated that the gene expression pattern in nephron precursors is more complex than previously thought. In particular, large-scale analysis of the expression of transcriptional

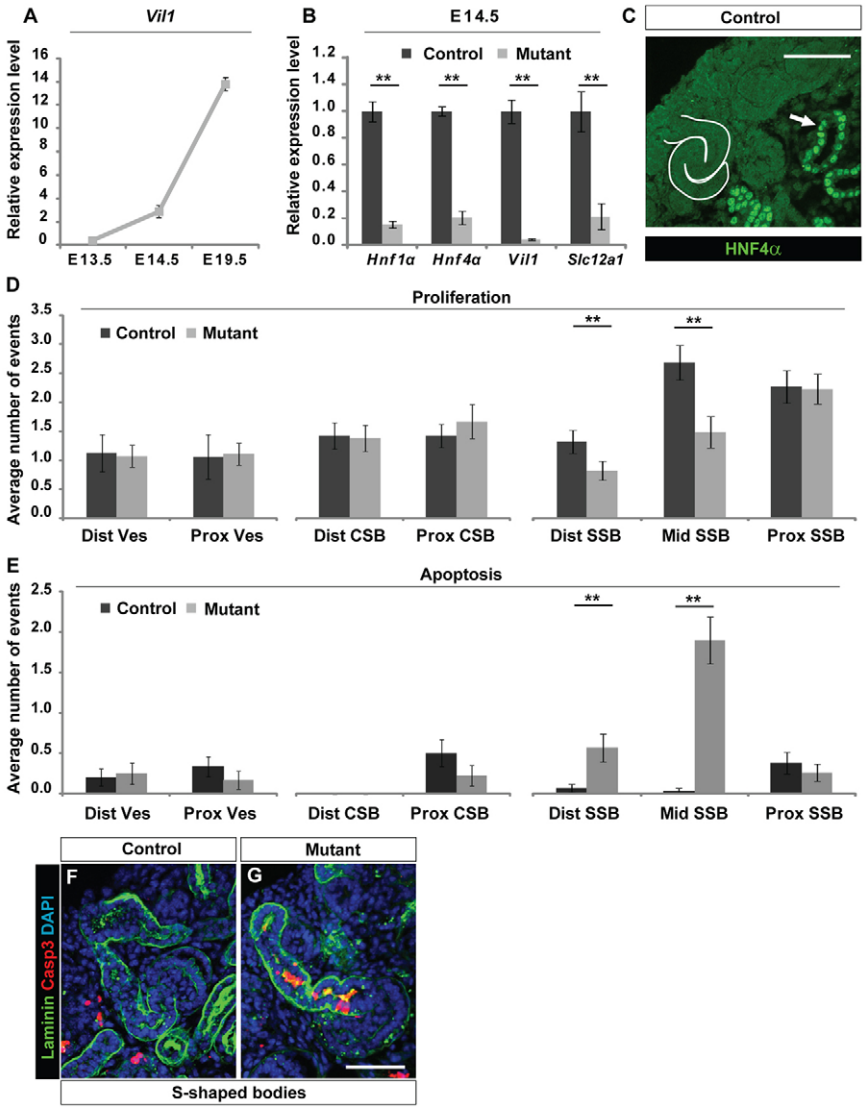

Fig. 3. The absence of tubule formation is not linked to a primary defect in proliferation or apoptosis in early nephron precursors. (**A**) qRT-PCR showing that in control embryos markers of the tubular differentiation program start to be expressed at low level at ~E14.5. (**B**) In mutant kidneys, already at this stage the expression of *Vil1*, *Hnf1a* and *Hnf4a* in the proximal tubule and *Slc12a1* in Henle's loop is drastically decreased. (**C**) Immunofluorescence with an anti-HNF4α antibody on a wild-type kidney section. HNF4α expression could not be detected in S-shaped bodies (white contour) and is only detected in already differentiated proximal tubules (arrow). (**D**,**E**) Proliferation/apoptosis balance in specific segments of nephron precursors. Semi-quantitative analysis of the number of mitotic (histone H3 PS10-positive) cells or apoptotic events (cleaved caspase-3-positive cells) relative to their location in subdomains of the developing nephron. Dist, distal; Prox, proximal; Ves, vesicles; CSB, comma-shaped bodies; SSB, S-shaped bodies (where Dist, Mid and Prox refer to upper, mid and lower limbs, respectively). For proliferation: Ves, control *n*=11 and mutant *n*=18; CSB, control *n*=25 and mutant *n*=21; SSB, control *n*=23 and mutant *n*=26. For apoptosis: Ves, control *n*=17 and mutant *n*=11; CSB, control *n*=18 and mutant *n*=19; SSB, control *n*=30 and mutant *n*=30. (**F**,**G**) Immunofluorescence with an anti-cleaved caspase-3 antibody showing representative images of apoptotic events in S-shaped bodies in control and mutant. ***P*<0.01; error bars indicate s.e.m. Scale bars: 25 μm.

regulatory factors has revealed novel molecular subdomains in developing renal structures (Thiagarajan et al., 2011; Yu et al., 2012). We took advantage of these findings in order to identify the specific nature of the deformation of S-shaped structures in mutant embryos. As a first approach, based on qRT-PCR analysis, we monitored genes that have been shown to be expressed in subdomains of the mid-limb, including *Osr2*, *Pou3f3* and *Irx1* (Yu et al., 2012). Our results showed significant downregulation in their expression already at E13.5 (Fig. 4A). In control embryos at this stage, *Cdh6* is predominantly expressed in renal vesicles. With the progressive appearance of comma- and S-shaped bodies, *Cdh6* also becomes specifically expressed in the first prospective PT precursor cells (Cho et al., 1998; Mah et al., 2000). In mutant embryos, *Cdh6* expression was normal at E13.5 but drastically decreased, together with *Osr2*, *Pou3f3* and *Irx1*, at E14.5 (Fig. 4B).

The mid-limb of S-shaped bodies is characterized by the expression of *Pou3f3* in a relatively large segment, whereas the expression patterns of *Osr2* and *Irx1* tend to be more restricted to the most proximal part of the mid-limb. ISH experiments revealed that the expression of these two genes was significantly reduced in mutant S-shaped bodies (Fig. 4C-F). In a similar way, using an immunohistochemical approach, we showed that the expression of *Jag1* was also decreased in the mid-limb of the S-shaped body (data not shown). In parallel, we also monitored the levels of expression of *Lhx1* and *Pax2*, genes that are known to be controlled by HNF1β in other kidney compartments (Lokmane et al., 2010) and that have been shown to play a role in kidney development (Dressler et al., 1993; Kobayashi et al., 2005). Our qRT-PCR analysis did not show any decreased expression of *Lhx1* or *Pax2* at E14.5 (Fig. 4K). At later steps, at E19.5, these two genes showed aberrant, persistently high expression in the abnormal S-shaped bodies of the mutant and in the rare and primitive tubular segments that were formed (Fig. 4G-J). In addition, qRT-PCR performed on newborn mutant pups showed clear upregulation of *Lhx1* and *Pax2* expression (Fig. 4K). The persistent expression of these genes suggests that, even if *Hnf1b* mutant embryos developed some short and primitive tubular components, they did not fully differentiate and still expressed markers of earlier steps of their developmental program.

It has been shown that Notch signaling plays a crucial role in the specification and differentiation of the most proximal structures of nephrons during development. Interestingly, mice carrying a hypomorphic allele of *Dll1*, one of the ligands of the Notch receptors, exhibit a phenotype reminiscent of that of our *Hnf1b* mutant embryos. In fact, the defective expression of *Dll1* leads to drastically reduced formation of PTs (Cheng et al., 2007). Interestingly, *Dll1*, Notch intracellular domain (NICD) and *Hes5*

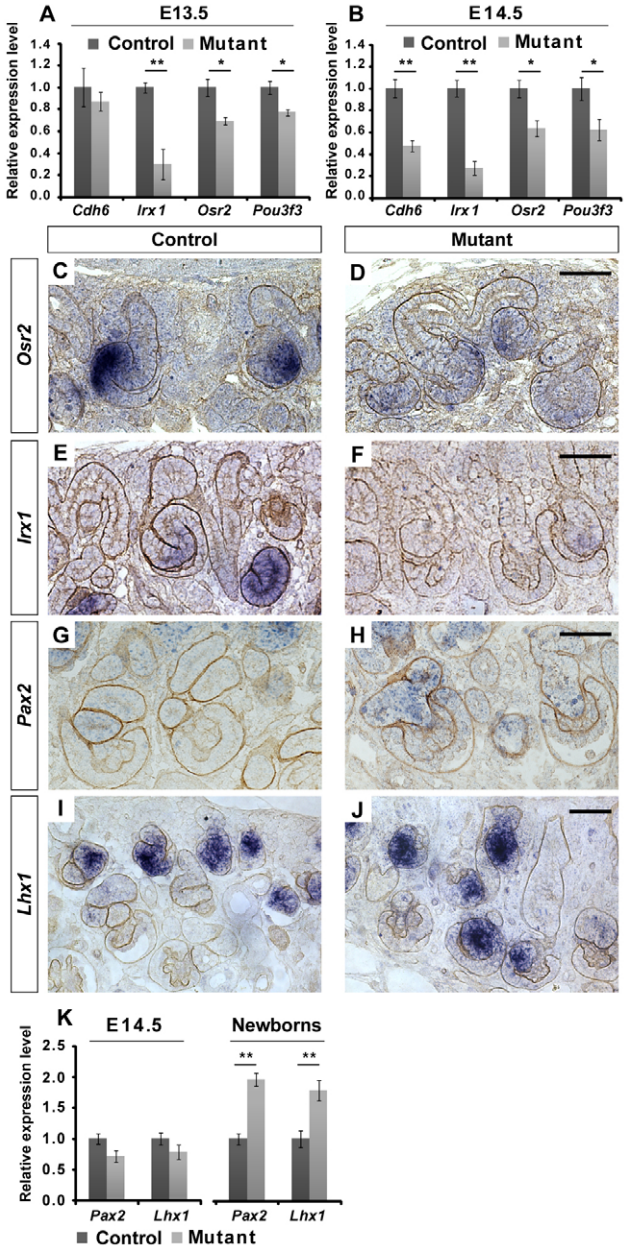

Fig. 4. Altered expression of markers of specific subdomains in nephron precursors of *Hnf1b* mutants. (**A**,**B**) qRT-PCR analysis of genes with particular patterns of expression in the mid-limb of S-shaped bodies at E13.5.and E14.5. (**C-J**) ISH on paraffin sections double labeled with an anti-laminin antibody. (C-F) In the *Hnf1b* mutant, *Osr2* and *Irx1* are downregulated in S-shaped bodies. (G-J) The high-level expression of *Pax2* and *Lhx1* in late nephron precursors was still detectable in the mutant compared with the control. (**K**) qRT-PCR analysis of expression of *Pax2* and *Lhx1* showing a similar expression level at E14.5 in mutant and control but an upregulation of expression at P0 in the mutant. **P*<0.05, ***P*<0.01; error bars indicate s.e.m. Scale bars: 25 μm.

are detected in the epithelial cells that form the bulge at the bend between the mid and lower limb of the S-shaped bodies (Cheng et al., 2007; Piscione et al., 2004).

We investigated the possible involvement of defective Notch signaling activation in the onset of the phenotypes observed in *Hnf1b* mutant embryonic kidneys. We first assessed the expression of *Notch2* and *Jag1*, key factors that have been shown to be controlled by HNF1α and HNF1β in the intestine (D'Angelo et al., 2010). qRT-PCR experiments showed that at E13.5 the expression of these two genes was similar in mutant and control embryonic kidneys (Fig. 5A). This level of expression was maintained at E14.5, with no differences between genotypes (Fig. 5B). By contrast, we saw significant downregulation of *Dll1* accompanied by significant downregulation of *Hes5*, one of the effector target genes of Notch signaling (Fig. 5A,B).

To assess the functional implication of Notch signaling pathway activation in the *Hnf1b* mutant phenotype we examined the possible genetic interaction between *Hnf1b* and *Notch2* in the specification and expansion of PTs. Our results showed that double heterozygous mice (*Hnf1b*$^{+/-}$; *Notch2*$^{+/-}$) at P0 had a modest but consistent reduction (~20%) of PTs compared with control animals (either wild-type or single-heterozygous mice; supplementary material Fig. S2). In a similar way, we also tested the possible genetic interaction between *Hnf1b* and *Pou3f3*. In this case, however, PT extents were similar in double-heterozygous and control newborns (data not shown).

In agreement with previous studies, our ISH experiments showed that *Dll1* is particularly strongly expressed in the epithelial bulge of control S-shaped bodies. We showed that this expression was drastically decreased in *Hnf1b* mutants (Fig. 5C,D). The defective expression of *Dll1* in mutants could have been ascribed to the lack of formation of this particular segment. Interestingly, *Dll1* is known to be expressed in earlier precursors, including vesicles and comma-shaped bodies, structures that apparently formed normally in our mutant embryos. When we assessed the expression of *Dll1* in these earlier structures, we could clearly see that *Dll1* was significantly downregulated in vesicles and comma-shaped bodies in mutant embryos (Fig. 5E-H). These results indicated that HNF1β is probably involved in the transcriptional activation of *Dll1* in nephron precursors.

HNF1β binds to several sites in the chromatin of crucial kidney development genes

To investigate whether *Dll1* could be directly controlled by HNF1β we assessed its direct binding *in vivo* by chromatin immunoprecipitation (ChIP) experiments on embryonic kidney chromatin. As a first step, we identified the position of the best candidate HNF1 binding sites using a previously described *in silico* approach (Verdeguer et al., 2010). This led to the identification of a particularly well conserved site 2 kb upstream of the transcription start site of the *Dll1* gene together with a second site much farther away (302 kb downstream). Our results showed that both sites are bound *in vivo* (supplementary material Fig. S3). The combination of the ISH and ChIP results suggests that the absence of bulge formation in *Hnf1b*-deficient kidneys might be a direct consequence of the defective expression of *Dll1* as a direct target of HNF1β already in early nephron precursors (vesicles and comma-shaped bodies).

Our *in silico* approach also led us to discover evolutionarily conserved HNF1 binding sites around the *Osr2* and *Irx1* genes. Our ChIP results showed that one site, detected close to *Osr2* (24.1 kb upstream of the putative transcription start site) and three sites around *Irx1* (14 kb, 65 kb and 66 kb upstream of the putative transcription start site), were significantly bound *in vivo* (supplementary material Fig. S3). Since expression of *Osr2* and *Irx1* is not detected in the deformed S-shaped bodies of *Hnf1b* mutants, one possibility is that their defective expression could simply be due to the absence of formation of their territory. However, we cannot rule out the possibility that the expansion of this crucial territory might also be controlled by HNF1β via the transcriptional activation of these two genes.

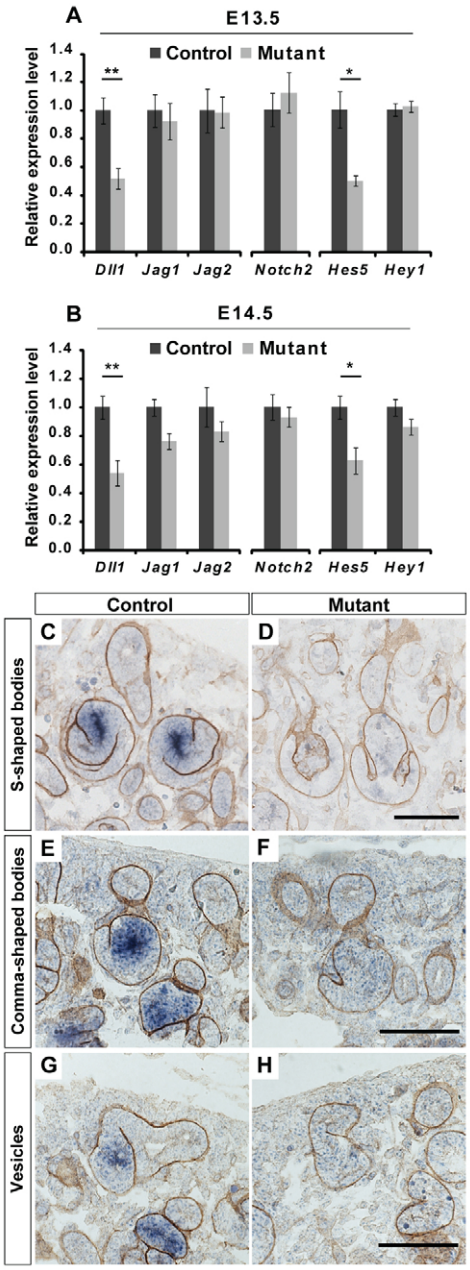

Fig. 5. The Notch pathway is affected by the absence of HNF1β in the metanephric mesenchyme. (**A**,**B**) qRT-PCR analysis of genes involved in the Notch signaling pathway at E13.5 and E14.5. (**C-H**) *Dll1* ISH on paraffin sections double labeled with an anti-laminin antibody. **P*<0.05, ***P*<0.01; error bars indicate s.e.m. Scale bars: 25 μm.

Glomerular phenotype induced by the absence of HNF1β

After the formation of S-shaped structures, the tubular components of the nephron normally proliferate and form their typical long tubules, including the PT, HL and DCT. In this respect, nephron spatial organization is characterized by the fact that the final portion of the HL ends with the macula densa, a tubular structure that is intimately connected with the vascular pole of the same glomerulus. The spatial organization of *Hnf1b*-deficient nephrons was characterized by a very short primitive tubule emerging from the glomerulus in continuation with the presumptive macula densa. Normally, the urinary pole of a glomerulus is located directly opposite (at 180 degrees) the vascular pole. In our mutant embryos, the absence of tubular expansion had probably led to a deformation of the glomeruli, such that the two poles were forced close to each other (Fig. 6A-C). In addition, the vascular tuft, instead of showing its typical constriction at its base (by the formation of the vascular pole), was characterized by an atypical distended conformation. In spite of this alteration, at the ultrastructural level the glomerular structures were globally normal, with podocytes and their foot processes surrounding capillaries with fenestrated endothelial cells (supplementary material Fig. S4). As mentioned above, mutant glomeruli had dilations of the Bowman's (urinary) space, forming glomerular cysts.

Altogether, these results showed that podocyte differentiation was unaltered but that the global architecture of the capillary tuft was distorted leading to a highly deformed global structure of the glomerulus.

The renal phenotype linked to human *HNF1B* deficiency

Fetuses carrying heterozygous mutations of *HNF1B* present with a set of complex and extremely variable renal abnormalities ranging from kidney agenesis to hypodysplasia and/or cysts (Decramer et al., 2007; Heidet et al., 2010). These abnormalities can be linked to an impaired differentiation process in MM-derived structures due to the defective expression of HNF1β and/or its target genes.

In an attempt to compare the pathological features observed in MODY5 patients with those in our mouse model, we analyzed paraffin sections from a MODY5 fetus (Patient 1) carrying a complete genomic deletion affecting all exons of *HNF1B*. Histological analysis of kidney sections revealed the presence of specific focal areas characterized by clusters of glomeruli, without their typical surrounding set of cortical convoluted tubules (Fig. 6D). Immunofluorescence experiments confirmed that there were only very few LTL-positive tubular sections (Fig. 6F). In addition, some of these glomerular structures were dilated and their capillary tuft was spread, similar to what was observed in the mutant mouse embryos (Fig. 6E,G). In addition, the analysis of paraffin sections from a MODY5 child (Patient 2) carrying a c.232G>T, p.Glu78X mutation showed the presence of glomerular cysts arranged next to one another and that lacked the typical surrounding tubular structures (Fig. 6H). In addition, we again observed the spreading of glomerular tufts that was typical of mutant mouse embryos (Fig. 6I).

DISCUSSION

Patients who carry *HNF1B* mutations (MODY5 patients) suffer from complex developmental dysfunction of kidney morphogenesis, including kidney agenesis, dysplasia and cyst formation (Decramer et al., 2007; Heidet et al., 2010; Ulinski et al., 2006). Previous studies indicated that the expression of *Hnf1b* in the UB of mouse embryonic kidneys is absolutely required for the expression of several key genes, including *Wnt9b*, which encodes an essential secreted factor for the condensation of the MM (Lokmane et al., 2010) (our unpublished observations). The absence of HNF1β in the UB leads to a complete block of nephrogenesis before the typical MET.

Very little is known about the role of HNF1β during the first steps of nephrogenesis, once the gene is programmed to be turned on in the mesenchyme-derived epithelial structures. In the present study, using a *Six2-Cre* inactivation strategy, we showed that the expression of HNF1β is not required for the first steps of nephron formation in mouse. The absence of this transcription factor does

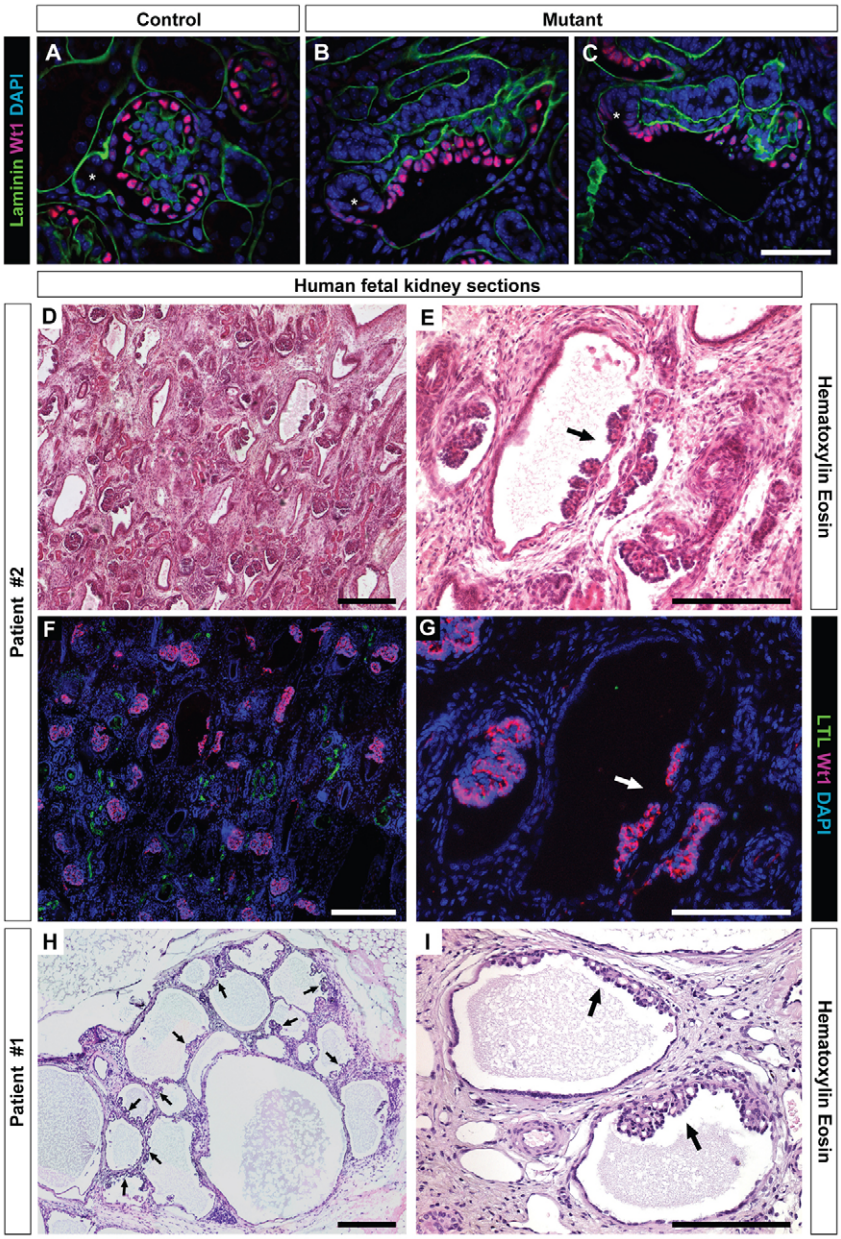

Fig. 6. The abnormal nephron conformation in *Hnf1b* mutant mouse embryos is reminiscent of the abnormalities in MODY5 patients. (**A-C**) Immunofluorescence of glomeruli on paraffin sections showing abnormal distended vascular tuft and glomerular cysts in mutant mouse embryos (B,C) compared with the control (A). Note that in mutant glomeruli the urinary pole (star in B,C) is in close connection with the vascular pole, as compared with its opposite localization in the control (star in A). (**D-I**) Histological analysis (D,E,H,I) and immunofluorescence (F,G) of paraffin kidney sections from a human MODY5 fetus (D-G) and from a MODY5 child (H,I) (images courtesy of Professor Laurent Daniel). A consistent number of glomeruli are visible on these sections, accompanied by very few LTL-positive tubular sections (F). Note the glomerular cysts, with a spread capillary tuft (arrows in E,G-I). Scale bars: 50 μm in A-C; 100 μm in D-I.

not perturb the typical formation and segmentation of renal vesicles and comma-shaped bodies. The first visible consequence of HNF1β deficiency becomes evident only in S-shaped bodies. In these structures, the most proximal portion of the mid-limb is deformed and the bulge of epithelial cells that probably contains the precursors of the PT and HL is missing (Fig. 7). This defect could be linked to the decreased expression of *Dll1*, as a hypomorphic *Dll1* allele can lead to defective expansion of renal tubules. We showed that *Dll1* expression is decreased in earlier nephron precursors (vesicles and comma-shaped bodies) before the appearance of any deformation (visible only in S-shaped bodies). In addition, our genetic interaction studies showed a modest but consistent reduction of proximal tubular expansion in *Notch2; Hnf1b* double-heterozygous newborns. Finally, HNF1β protein binds to the transcriptional control regions of the *Dll1* gene *in vivo*. All these considerations suggest that HNF1β might indeed play an important role in the expression of *Dll1*. It is worth noting that the phenotype of our *Hnf1b* mutant overlaps only partially with that induced by the deletion of *Notch2* (Cheng et al., 2007). In fact, *Notch2* mutant embryos completely lack the most proximal part of the nephron including the PT and glomeruli. In addition, HNF1β is required for the differentiation and expansion of DCTs, a process that does not require *Notch2* (Cheng et al., 2007). Altogether, these considerations indicate that the transcription factor HNF1β is involved in the formation of all nephron tubular components.

Analysis of the phenotype of mesenchyme-specific *Hnf1b*-deficient kidneys showed that PTs and HL formation seems to derive from a specific subdomain of S-shaped bodies. This process, which is promoted via the activation of Notch signaling, leads to the specification of a set of cells, probably already in the comma-shaped body. Expansion in the number of these cells gives rise to a particular territory in the more proximal part of the mid-segment of the S-shaped body. This particular subdomain of the S-shaped body, which is organized as a protruding bulge of epithelial cells, is probably at the origin of the future expansion of the whole tubular component of the nephron between the glomerulus and the macula densa. At the

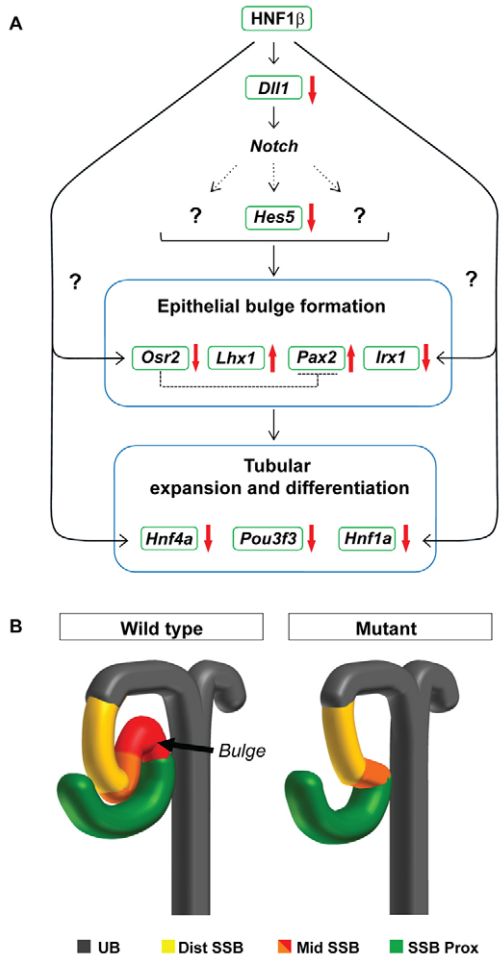

Fig. 7. Models depicting the function of HNF1β in nephron tubule formation. (**A**) HNF1β directly controls the expression of *Dll1* in early nephron precursors. *Dll1*, through Notch signaling, activates the specification of the epithelial bulge at the junction between the mid and lower limbs in S-shaped bodies. This particular territory will express a set of markers that may participate in the further steps of tubular expansion and differentiation. Genes that have been shown to be modulated in their expression in the absence of *Hnf1b* in metanephric mesenchyme are indicated by a red arrow representing up- or downregulation. (**B**) Schematic structure of wild-type and mutant S-shaped bodies. The bulge of epithelial cells (arrow) that is present in the wild type at the junction of the mid and lower limbs does not emerge in the *Hnf1b* mutant. UB, ureteric bud; SSB; S-shaped body.

molecular level, specific markers are expressed in this particular domain of the S-shaped body, such as *Osr2* and *Irx1*. Interestingly, the downregulation of *Irx1* in *Xenopus* leads to abnormal morphogenesis of the intermediate pronephric tubules (Alarcón et al., 2008). In parallel, *Osr2* has been shown to be involved in proximal segment differentiation in *Xenopus* and zebrafish (Tena et al., 2007), but its role in mammalian kidney morphogenesis is probably redundant as its inactivation in mouse does not lead to any renal abnormality (Lan et al., 2004). Interestingly, Osr2 been shown to act as a repressor that negatively regulates the expression of *Pax2* in zebrafish and *Xenopus* (Tena et al., 2007). This property might explain the persistently high expression of *Pax2* observed in the primitive tubules of mutant embryos. Even if the defective expression of *Irx1* and *Osr2* does not play any direct causal role in our *Hnf1b* mutant mouse phenotype, the presence of evolutionarily conserved HNF1 binding sites that are bound *in vivo* suggests that they could constitute a direct transcriptional cascade that could participate in the differentiation and expansion of tubules in combination with the role played by HNF1β at later steps of differentiation (Fig. 7).

Hnf1b-deficient S-shaped structures can generate a glomerulus with podocytes that can reach maturity with the development of normal foot processes. This observation is somewhat compatible with the fact that HNF1β is not expressed in podocytes and their precursors. The only proximal nephron structure that expresses HNF1β is the Bowman's capsule. In this context, we observed some dilation of the Bowman's (urinary) space and the formation of glomerular cysts. This glomerulocystic phenotype is observed with variable penetrance in MODY5 patients who carry mutations in *HNF1B* in the heterozygous state (Bingham et al., 2001). Intriguingly, in mouse, the heterozygous inactivation of *Hnf1b* does not cause any significant phenotype unless mice carry compound heterozygosity for both *Hnf1b* and other transcription factors (Paces-Fessy et al., 2012). However, the complete deletion of *Hnf1b* in either the UB or in the mesenchyme or in already formed tubules gives rise to the same traits that are observed in MODY5 patients with variable penetrance. This indicates that, somehow, the haploinsufficiency in MODY5 patients might reduce the protein levels below a critical threshold. This could lead to the appearance of a phenotype in the UB leading to defective branching and MET (hypodysplasia). In addition, haploinsufficiency in already formed nephron precursors could lead to defective tubular expansion accompanied by glomerular cysts. These phenotypes are recapitulated in mouse embryo models in which it has been demonstrated that HNF1β controls the expression of crucial effectors of kidney morphogenesis. Interestingly, the inactivation of *Hnf1b* in nephron progenitors using a Wnt4-Cre line and another *Hnf1b* floxed allele gave rise to the same phenotype. This confirms the crucial role of HNF1β in nephron tubular specification (Heliot et al., 2013).

In conclusion, our studies have demonstrated that HNF1β plays an essential role in the generation of renal tubules. In particular, HNF1β is required for the formation of a specific mid-limb subcompartment (epithelial bulge) of S-shaped bodies, which is probably at the origin of the expansion of PTs and HLs via the activation of a set of crucial kidney development genes (Fig. 7).

Acknowledgements
We thank Moshe Yaniv for helpful discussions and critical reading of the manuscript; Professor Laurent Daniel (CHU Timone, Marseille, France) for providing images of histological sections of a kidney from a MODY5 patient; and Raphael Kopan for providing *Notch2* mouse models. We thank Silvia Cereghini for sharing unpublished data. We are very grateful to the platform of Imagerie Cellulaire, Morphologie et Histologie and the animal house facilities of the Cochin Institute.

Funding
This work was supported by the Fondation pour la Recherche Médicale (equipe FRM) and the Fondation Bettencourt-Schueller (Prix Coup d'Elan); European Community's Seventh Framework Programme FP7/2009 [agreement no: 241955, SYSCILIA]; and Agence National pour la Recherche. F.M. was supported by Société de Néphrologie, Association Polykystose France and Fondation pour la Recherche Médicale fellowships.

Competing interests statement
The authors declare no competing financial interests.

Supplementary material
Supplementary material available online at
http://dev.biologists.org/lookup/suppl/doi:10.1242/dev.086546/-/DC1

References

Alarcón, P., Rodríguez-Seguel, E., Fernández-González, A., Rubio, R. and Gómez-Skarmeta, J. L. (2008). A dual requirement for Iroquois genes during *Xenopus* kidney development. *Development* **135**, 3197-3207.

Barbacci, E., Reber, M., Ott, M. O., Breillat, C., Huetz, F. and Cereghini, S. (1999). Variant hepatocyte nuclear factor 1 is required for visceral endoderm specification. *Development* **126**, 4795-4805.

Bingham, C., Bulman, M. P., Ellard, S., Allen, L. I., Lipkin, G. W., Hoff, W. G., Woolf, A. S., Rizzoni, G., Novelli, G., Nicholls, A. J. et al. (2001). Mutations in the hepatocyte nuclear factor-1beta gene are associated with familial hypoplastic glomerulocystic kidney disease. *Am. J. Hum. Genet.* **68**, 219-224.

Bohn, S., Thomas, H., Turan, G., Ellard, S., Bingham, C., Hattersley, A. T. and Ryffel, G. U. (2003). Distinct molecular and morphogenetic properties of mutations in the human HNF1beta gene that lead to defective kidney development. *J. Am. Soc. Nephrol.* **14**, 2033-2041.

Boyle, S. C., Kim, M., Valerius, M. T., McMahon, A. P. and Kopan, R. (2011). Notch pathway activation can replace the requirement for Wnt4 and Wnt9b in mesenchymal-to-epithelial transition of nephron stem cells. *Development* **138**, 4245-4254.

Carroll, T. J., Park, J. S., Hayashi, S., Majumdar, A. and McMahon, A. P. (2005). Wnt9b plays a central role in the regulation of mesenchymal to epithelial transitions underlying organogenesis of the mammalian urogenital system. *Dev. Cell* **9**, 283-292.

Cheng, H. T., Kim, M., Valerius, M. T., Surendran, K., Schuster-Gossler, K., Gossler, A., McMahon, A. P. and Kopan, R. (2007). Notch2, but not Notch1, is required for proximal fate acquisition in the mammalian nephron. *Development* **134**, 801-811.

Cho, E. A., Patterson, L. T., Brookhiser, W. T., Mah, S., Kintner, C. and Dressler, G. R. (1998). Differential expression and function of cadherin-6 during renal epithelium development. *Development* **125**, 803-812.

Coffinier, C., Barra, J., Babinet, C. and Yaniv, M. (1999a). Expression of the vHNF1/HNF1beta homeoprotein gene during mouse organogenesis. *Mech. Dev.* **89**, 211-213.

Coffinier, C., Thépot, D., Babinet, C., Yaniv, M. and Barra, J. (1999b). Essential role for the homeoprotein vHNF1/HNF1beta in visceral endoderm differentiation. *Development* **126**, 4785-4794.

Coffinier, C., Gresh, L., Fiette, L., Tronche, F., Schütz, G., Babinet, C., Pontoglio, M., Yaniv, M. and Barra, J. (2002). Bile system morphogenesis defects and liver dysfunction upon targeted deletion of HNF1beta. *Development* **129**, 1829-1838.

D'Angelo, A., Bluteau, O., Garcia-Gonzalez, M. A., Gresh, L., Doyen, A., Garbay, S., Robine, S. and Pontoglio, M. (2010). Hepatocyte nuclear factor 1alpha and beta control terminal differentiation and cell fate commitment in the gut epithelium. *Development* **137**, 1573-1582.

Decramer, S., Parant, O., Beaufils, S., Clauin, S., Guillou, C., Kessler, S., Aziza, J., Bandin, F., Schanstra, J. P. and Bellanné-Chantelot, C. (2007). Anomalies of the TCF2 gene are the main cause of fetal bilateral hyperechogenic kidneys. *J. Am. Soc. Nephrol.* **18**, 923-933.

Dressler, G. R. (2009). Advances in early kidney specification, development and patterning. *Development* **136**, 3863-3874.

Dressler, G. R., Wilkinson, J. E., Rothenpieler, U. W., Patterson, L. T., Williams-Simons, L. and Westphal, H. (1993). Deregulation of Pax-2 expression in transgenic mice generates severe kidney abnormalities. *Nature* **362**, 65-67.

Fischer, E., Legue, E., Doyen, A., Nato, F., Nicolas, J. F., Torres, V., Yaniv, M. and Pontoglio, M. (2006). Defective planar cell polarity in polycystic kidney disease. *Nat. Genet.* **38**, 21-23.

Georgas, K., Rumballe, B., Wilkinson, L., Chiu, H. S., Lesieur, E., Gilbert, T. and Little, M. H. (2008). Use of dual section mRNA *in situ* hybridisation/immunohistochemistry to clarify gene expression patterns during the early stages of nephron development in the embryo and in the mature nephron of the adult mouse kidney. *Histochem. Cell Biol.* **130**, 927-942.

Gresh, L., Fischer, E., Reimann, A., Tanguy, M., Garbay, S., Shao, X., Hiesberger, T., Fiette, L., Igarashi, P., Yaniv, M. et al. (2004). A transcriptional network in polycystic kidney disease. *EMBO J.* **23**, 1657-1668.

Harding, S. D., Armit, C., Armstrong, J., Brennan, J., Cheng, Y., Haggarty, B., Houghton, D., Lloyd-MacGilp, S., Pi, X., Roochun, Y. et al. (2011). The GUDMAP database – an online resource for genitourinary research. *Development* **138**, 2845-2853.

Heidet, L., Decramer, S., Pawtowski, A., Morinière, V., Bandin, F., Knebelmann, B., Lebre, A. S., Faguer, S., Guigonis, V., Antignac, C. et al. (2010). Spectrum of HNF1B mutations in a large cohort of patients who harbor renal diseases. *Clin. J. Am. Soc. Nephrol.* **5**, 1079-1090.

Heliot, C., Desgrange, A., Buisson, I., Prunskaite-Hyyryläinen, R., Shan, J., Vainio, S., Umbhauer, M. and Cereghini, S. (2013). HNF1B controls proximal-intermediate nephron segment identity in vertebrates by regulating Notch signalling components and *Irx1/2*. *Development* **140**, 873-885.

Hiesberger, T., Bai, Y., Shao, X., McNally, B. T., Sinclair, A. M., Tian, X., Somlo, S. and Igarashi, P. (2004). Mutation of hepatocyte nuclear factor-1beta inhibits Pkhd1 gene expression and produces renal cysts in mice. *J. Clin. Invest.* **113**, 814-825.

Horikawa, Y., Iwasaki, N., Hara, M., Furuta, H., Hinokio, Y., Cockburn, B. N., Lindner, T., Yamagata, K., Ogata, M., Tomonaga, O. et al. (1997). Mutation in hepatocyte nuclear factor-1 beta gene (TCF2) associated with MODY. *Nat. Genet.* **17**, 384-385.

Humphreys, B. D., Valerius, M. T., Kobayashi, A., Mugford, J. W., Soeung, S., Duffield, J. S., McMahon, A. P. and Bonventre, J. V. (2008). Intrinsic epithelial cells repair the kidney after injury. *Cell Stem Cell* **2**, 284-291.

Kobayashi, A., Kwan, K. M., Carroll, T. J., McMahon, A. P., Mendelsohn, C. L. and Behringer, R. R. (2005). Distinct and sequential tissue-specific activities of the LIM-class homeobox gene Lim1 for tubular morphogenesis during kidney development. *Development* **132**, 2809-2823.

Kobayashi, A., Valerius, M. T., Mugford, J. W., Carroll, T. J., Self, M., Oliver, G. and McMahon, A. P. (2008). Six2 defines and regulates a multipotent self-renewing nephron progenitor population throughout mammalian kidney development. *Cell Stem Cell* **3**, 169-181.

Lan, Y., Ovitt, C. E., Cho, E. S., Maltby, K. M., Wang, Q. and Jiang, R. (2004). Odd-skipped related 2 (Osr2) encodes a key intrinsic regulator of secondary palate growth and morphogenesis. *Development* **131**, 3207-3216.

Lindner, T. H., Njolstad, P. R., Horikawa, Y., Bostad, L., Bell, G. I. and Sovik, O. (1999). A novel syndrome of diabetes mellitus, renal dysfunction and genital malformation associated with a partial deletion of the pseudo-POU domain of hepatocyte nuclear factor-1beta. *Hum. Mol. Genet.* **8**, 2001-2008.

Lokmane, L., Heliot, C., Garcia-Villalba, P., Fabre, M. and Cereghini, S. (2010). vHNF1 functions in distinct regulatory circuits to control ureteric bud branching and early nephrogenesis. *Development* **137**, 347-357.

Mah, S. P., Saueressig, H., Goulding, M., Kintner, C. and Dressler, G. R. (2000). Kidney development in cadherin-6 mutants: delayed mesenchyme-to-epithelial conversion and loss of nephrons. *Dev. Biol.* **223**, 38-53.

McMahon, A. P., Aronow, B. J., Davidson, D. R., Davies, J. A., Gaido, K. W., Grimmond, S., Lessard, J. L., Little, M. H., Potter, S. S., Wilder, E. L. et al. (2008). GUDMAP: the genitourinary developmental molecular anatomy project. *J. Am. Soc. Nephrol.* **19**, 667-671.

Nakai, S., Sugitani, Y., Sato, H., Ito, S., Miura, Y., Ogawa, M., Nishi, M., Jishage, K., Minowa, O. and Noda, T. (2003). Crucial roles of Brn1 in distal tubule formation and function in mouse kidney. *Development* **130**, 4751-4759.

Paces-Fessy, M., Fabre, M., Lesaulnier, C. and Cereghini, S. (2012). Hnf1b and Pax2 cooperate to control different pathways in kidney and ureter morphogenesis. *Hum. Mol. Genet.* **21**, 3143-3155.

Piscione, T. D., Wu, M. Y. and Quaggin, S. E. (2004). Expression of Hairy/Enhancer of Split genes, Hes1 and Hes5, during murine nephron morphogenesis. *Gene Expr. Patterns* **4**, 707-711.

Rumballe, B., Georgas, K., Wilkinson, L. and Little, M. (2010). Molecular anatomy of the kidney: what have we learned from gene expression and functional genomics? *Pediatr. Nephrol.* **25**, 1005-1016.

Stark, K., Vainio, S., Vassileva, G. and McMahon, A. P. (1994). Epithelial transformation of metanephric mesenchyme in the developing kidney regulated by Wnt-4. *Nature* **372**, 679-683.

Sun, Z., Amsterdam, A., Pazour, G. J., Cole, D. G., Miller, M. S. and Hopkins, N. (2004). A genetic screen in zebrafish identifies cilia genes as a principal cause of cystic kidney. *Development* **131**, 4085-4093.

Tan, J. B., Xu, K., Cretegny, K., Visan, I., Yuan, J. S., Egan, S. E. and Guidos, C. J. (2009). Lunatic and manic fringe cooperatively enhance marginal zone B cell precursor competition for delta-like 1 in splenic endothelial niches. *Immunity* **30**, 254-263.

Tena, J. J., Neto, A., de la Calle-Mustienes, E., Bras-Pereira, C., Casares, F. and Gómez-Skarmeta, J. L. (2007). Odd-skipped genes encode repressors that control kidney development. *Dev. Biol.* **301**, 518-531.

Thiagarajan, R. D., Georgas, K. M., Rumballe, B. A., Lesieur, E., Chiu, H. S., Taylor, D., Tang, D. T., Grimmond, S. M. and Little, M. H. (2011). Identification of anchor genes during kidney development defines ontological relationships, molecular subcompartments and regulatory pathways. *PLoS ONE* **6**, e17286.

Tronche, F., Ringeisen, F., Blumenfeld, M., Yaniv, M. and Pontoglio, M. (1997). Analysis of the distribution of binding sites for a tissue-specific transcription factor in the vertebrate genome. *J. Mol. Biol.* **266**, 231-245.

Ulinski, T., Lescure, S., Beaufils, S., Guigonis, V., Decramer, S., Morin, D., Clauin, S., Deschênes, G., Bouissou, F., Bensman, A. et al. (2006). Renal phenotypes related to hepatocyte nuclear factor-1beta (TCF2) mutations in a pediatric cohort. *J. Am. Soc. Nephrol.* **17**, 497-503.

Verdeguer, F., Le Corre, S., Fischer, E., Callens, C., Garbay, S., Doyen, A., Igarashi, P., Terzi, F. and Pontoglio, M. (2010). A mitotic transcriptional switch in polycystic kidney disease. *Nat. Med.* **16**, 106-110.

Wu, G., Bohn, S. and Ryffel, G. U. (2004). The HNF1beta transcription factor has several domains involved in nephrogenesis and partially rescues Pax8/lim1-induced kidney malformations. *Eur. J. Biochem.* **271**, 3715-3728.

Yu, J., Valerius, M. T., Duah, M., Staser, K., Hansard, J. K., Guo, J. J., McMahon, J., Vaughan, J., Faria, D., Georgas, K. et al. (2012). Identification of molecular compartments and genetic circuitry in the developing mammalian kidney. *Development* **139**, 1863-1873.

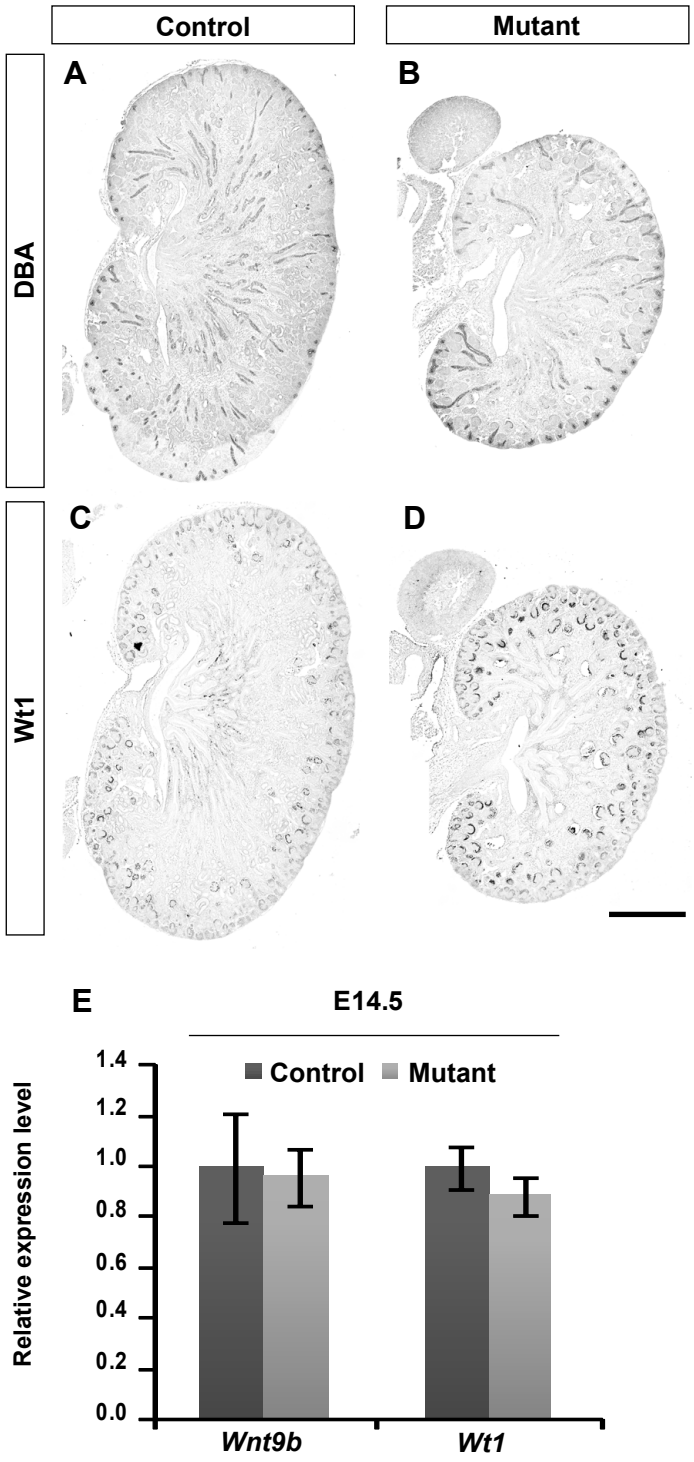

Fig. S1. The absence of HNF1β in metanephric mesenchyme does not affect UB branching and podocyte differentiation. (**A-C**) Kidney sections of newborns from control and mutant showed a similar staining for collecting ducts with Dolicho biflorus agglutinin (DBA) (A,B) and for Wt1 (C,D). (**E**) qRT-PCR analysis of specific markers of collecting ducts (*Wnt9b*) and podocytes (*Wt1*) did not show any difference between control and mutant kidneys at E14.5. Scale bar: 500 μm.

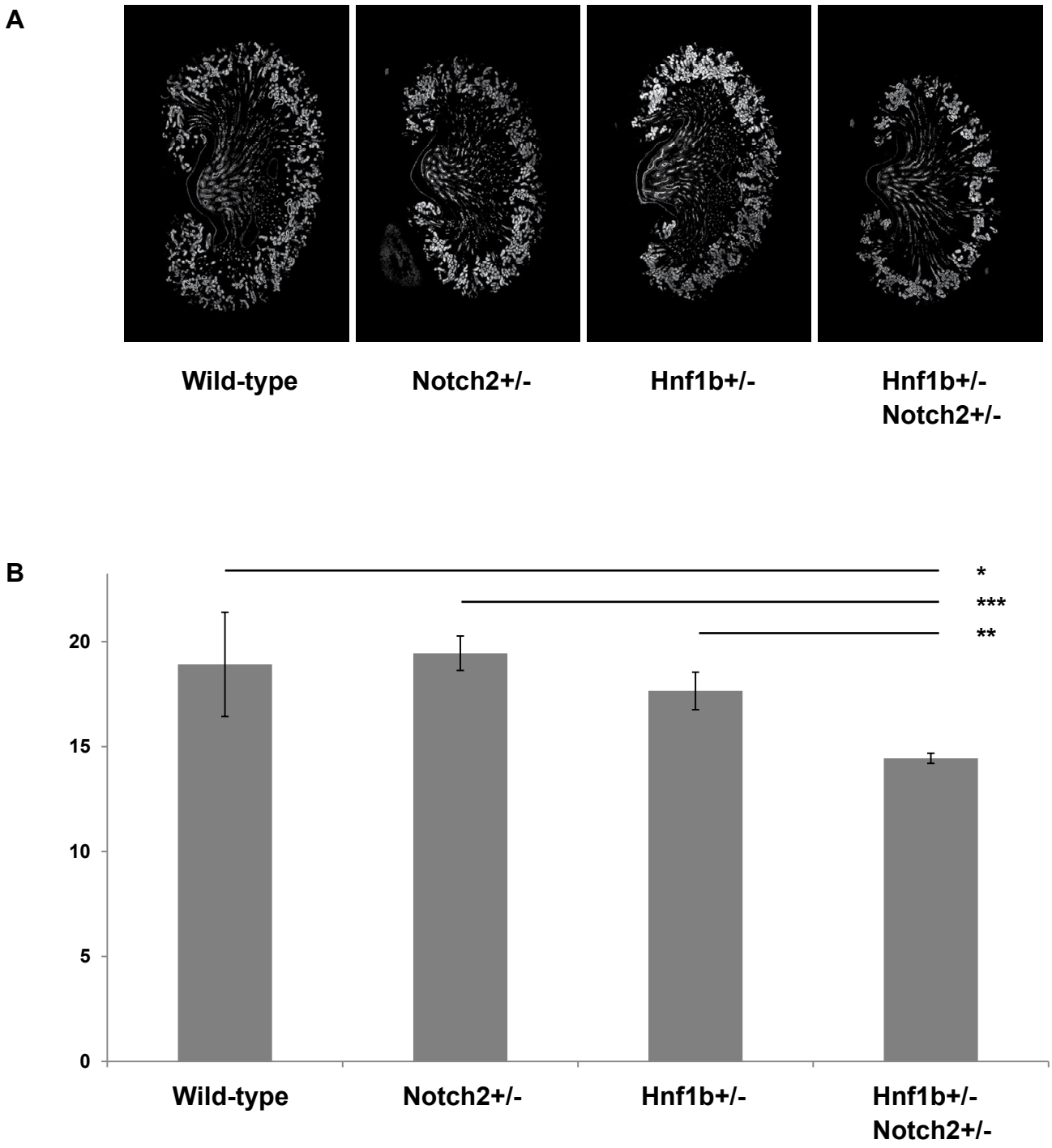

Fig. S2. Genetic interaction between *Hnf1b* and *Notch2* in proximal tubule expansion. (**A**) Immunofluorescence detection of *Lotus tetragonolobus* lectin (LTL; proximal tubules) showing the slight decrease in expansion of proximal tubules in double-heterozygous pups (*Notch2*$^{+/-}$*; Hnf1b*$^{+/-}$). (**B**) Quantification of the relative (percentage) surface of proximal tubules per kidney section. *n*=3, 5, 4 and 6 for wild type, *Notch2*$^{+/-}$, *Hnf1b*$^{+/-}$ and *Hnf1b*$^{+/-}$*; Notch2*$^{+/-}$, respectively. Student's *t*-test: **P*=0.015, ***P*=0.0015, ****P*<0.001.

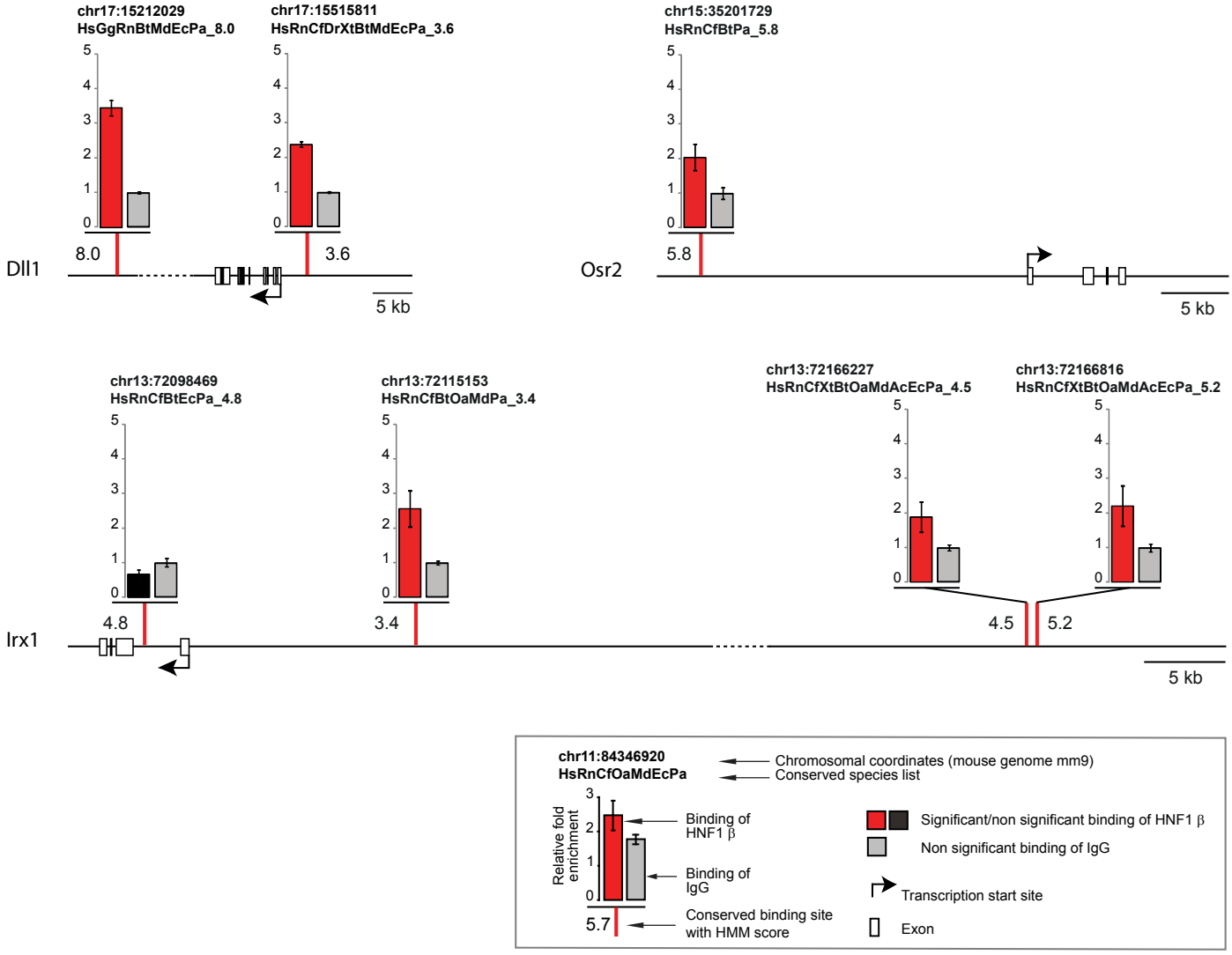

Fig. S3. In vivo binding of HNF1β to its chromatin target sites in genes involved in tubular differentiation. Predicted *in silico* HNF1 binding sites (vertical bars) in *Dll1*, *Osr2* and *Irx1* genes were tested in ChIP experiments for *in vivo* HNF1β binding. The relative enrichment for each DNA fragment upon immunoprecipitation of HNF1β is illustrated in histograms. Colored bars represent HNF1 binding sites with enrichments significantly higher than background (gray bars). PCR experiments were performed in triplicate and the standard errors of these quantifications are shown as error bars. Species list of conserved sites: Ac, *Anolis carolinensis*; Bt, *Bos taurus*; Cf, *Canis familiaris*; Dr, *Danio rerio*; Ec, *Equus caballus*; Gg, *Gallus gallus*; Hs, *Homo sapiens*; Md, *Monodelphis domestica*; Oa, *Ornithorhynchus anatinus*; Pa, *Pongo pygmaeus abelii*; Rn, *Rattus norvegicus*; Xt, *Xenopus tropicalis*.

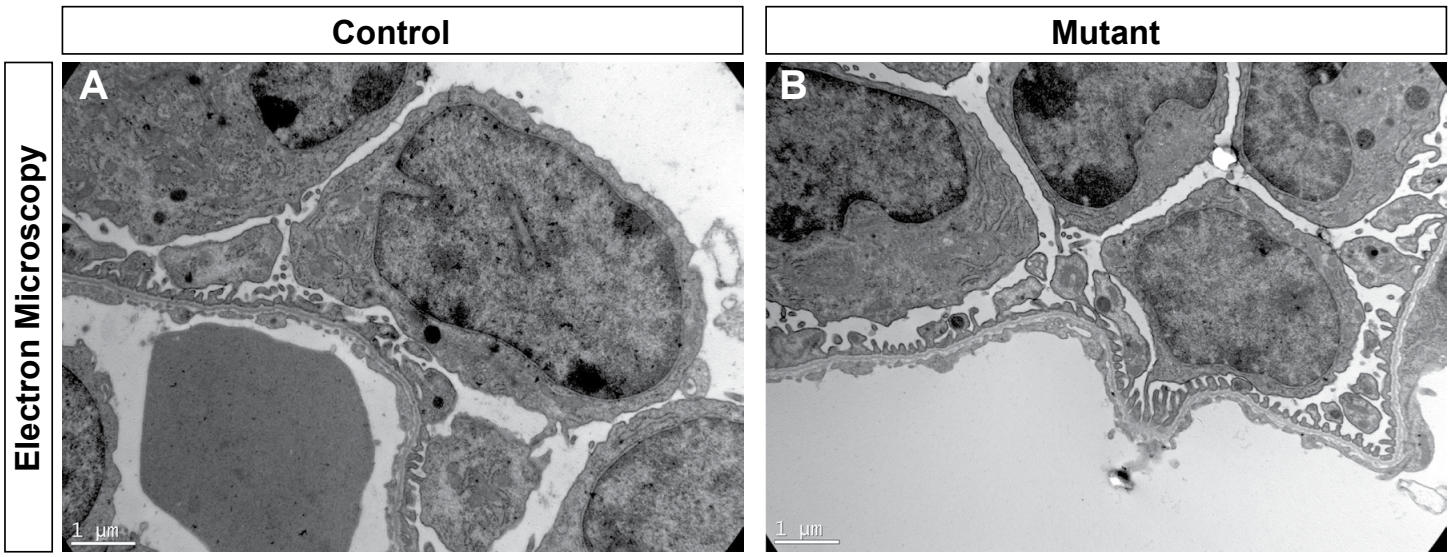

Fig. S4. Podocytes develop normally in the absence of HNF1β. Transmission electron microscopy of glomerular sections showing similar extent of foot process differentiation in podocytes of control (**A**) and mutant (**B**) newborn pups.

Table S1. Antibodies

Host species	Target protein	Source	Dilution
Mouse	WT1	Dako (M356101)	1:100
Rabbit	Laminin	Sigma (L9393)	1:200
Rabbit	HNF4α	FRH4 (homemade)	1:100
Rabbit	JAG1	Santa Cruz (SC-8303)	1:200
–	*Lotus tetragonolobus* lectin (LTL)	Vector (B-1325)	1:200
–	*Dolichos biflorus* agglutinin (DBA)	Vector (B-1035)	1:200
Mouse	HNF1β	HNF1b-3-12 (homemade)	1:100

Table S2. qRT-PCR primers

Gene	Primer	Sequence
Vil1	Reverse	GCGAGACTTTCCGGAGCTACT
	Forward	CCCCTTTCCGGATCACAAG
Hnf4a	Reverve	ATCACCTGGCAGATGATCGAA
	Forward	AGGTTGTCAATCTTGGCCATG
Slc12a1	Reverse	CTGGCCTCATATGCGCTTATT
	Forward	AGATTTGGCATACGAGGCATG
Slc12a3	Reverse	GGCCTACGAACACTATGCTAAC
	Forward	AGTCAGCTCACGACCTTGC
Pvalb	Reverse	CAGACTCCTTCGACCACAAAAA
	Forward	AACCCCAATCTTGCCGTCC
Dll1	Reverse	GAACAACCTAGCCAATTGCCA
	Forward	GCCCCAATGATGCTAACAGAA
Jag1	Reverse	ACTCGGAAGTGGAGGAGGATG
	Forward	AGCGGACTTTCTGCTGGTGT
Jag2	Reverse	CAATGCTGAGCCTGACCAATAC
	Forward	GACGGACAGTGGCATTCAAA
Notch2	Reverse	CCCTGATCATCGTGGTGCT
	Forward	AATGCGCAAGTTGGTGTGG
Hes5	Reverse	TCAACAGCAGCATAGAGCAGC
	Forward	TCCAGGATGTCGGCCTTCT
Hey1	Reverse	CCGACGAGACCGAATCAATAAC
	Forward	TCAGGTGATCCACAGTCATCTG
Cdh6	Reverse	CTAGTGGCTTCCCAGCAAAG
	Forward	CTGATAATCGGATCCCGTGT
Pou3f3	Reverse	CAGCCTACAGCTGGAAAAGG

	Forward	GGTACCCACCTGCGAGTAGA
Hnf1a	Reverse	AACCACCCTCTCTCCCAGTAA
	Forward	GCCGCAGACACTGTGACTAA
Osr2	Reverse	CCACGGACTGTACACCTGTC
	Forward	GAAAGATCGCATGTTCAGCA
Irx1	Reverse	ATTCACGAGAGGACCCACAC
	Forward	TCCTTTCCCACACTCCTGAC
Pax2	Reverse	CAAAGTTCAGCAGCCTTTCC
	Forward	GTTAGAGGCGCTGGAAACAG
Lhx1	Reverse	TGCGTCCAGTGCTGTGAAT
	Forward	AACCAGATCGCTTGGAGAGAT
Wt1	Reverse	GGTTTTCTCGCTCAGACCAG
	Forward	GGTGTGGGTCTTCAGATGGT
Wnt9b	Reverse	GTGAGGTCCTGACACCCTTC
	Forward	GCCTGGACAGCTTCAGTAGG

Table S3. ISH probe primers

Gene	Primer	Sequence
Osr2	Reverse	GCTGCAGCTCACCAATTACTCC
	Forward	ACTTTGCCGCACTGCTCGCAGC
Irx1	Reverse	ACCCTCACACAGGTCTCCAC
	Forward	GGAAAGATCGCATGTTCAGCA
Dll1	Reverse	CTAGAACACTCTGGGAGCGG
	Forward	GTCTTCAAAGACCCAGGGATG
Lhx1	Reverse	ACAAATGGTTCCCGTAGCTG
	Forward	CAACATGCGTGTTATCCAGG
Pvalb	Reverse	CTGGAGAACCTGTTCGCTTC
	Forward	CAGAGGCATCTCTCACCACA
Slc12a1	Reverse	CTGGTATGGTGAAGGCAGGT
	Forward	CAAACCAAAAGCAAGCCATT

Table S4. ChIP primers

Gene	Sites	Primer	Sequence
Dll1	17_15515811_HsRnCfDrXtBtMdEcPa_3.6 chr17:15515812-15515826	Reverse	AGGGTCTGAGCTATGCTTGC
		Forward	GCTGTGTCCAACAGGGACTT
	17_15212029_HsGgRnBtMdEcPa_8.0 chr17:15212030-15212044	Reverse	AAGAGCGGCCTCAGTCATTA
		Forward	CAGACCATAGCCACAGGACA
Irx1	13_72166227_HsRnCfXtBtOaMdAcEcPa_4.5	Reverse	ACTCATGCCTGCGATAATCC

	chr13:72166228-72166242	Forward	TTCCCACCAACCTCATTTTC
	13_72166816_HsRnCfXtBtOaMdAcEcPa_5.2	Reverse	CGGCTGCTAATCCAGTGTCT
	chr13:72166817-72166831	Forward	GGGAGGACTTTCTCCTGTCC
	13_72115153_HsRnCfBtOaMdPa_3.4	Reverse	ATGATGGTTCCAGGCTGTTC
	chr13:72115154-72115168	Forward	TGTGTGGATTGCTCATGGAT
	13_72098469_HsRnCfBtEcPa_4.8	Reverse	TCCAGGGCACTCTTCAGTCT
	chr13:72098470-72098484	Forward	ACCTGTCACCGCTACAGACC
Osr2	15_35201729_HsRnCfBtPa_5.8	Reverse	ATGCTGGCCTTTTATGTTGC
	chr15:35201730-35201744	Forward	TGTGGGAAAATCAGACAGCA